Preliminary Design of a PEM Fuel Cell Simulator Based on Digitally Controlled DC-DC Buck Converter

Goce L. Arsov, Georgi Georgievski

***Abstract*—Modeling of fuel cells is getting more and more important as power fuel cell stacks being available and have to be integrated into real power systems. This paper presents a novel circuit model for a PEM fuel cell that can be used to design fuel cell simulator. The model is consisted of a DC-DC buck converter driven by PIC 16F877 microcontroller. The model can be used in design and analysis of fuel cell power systems by simulation or by using practically realized simulator.**

***Index Terms*—PEM Fuel cell, Modeling, Simulation, Pulse Width Modulation (PWM).**

I. Introduction

FUEL cells as energy source have been present since 1839. They were discovered and developed by the English physicist William Grove. But, since then, for more over one century they were not more than a laboratory curiosity [1]. After the period of 120 years since the fuel cells emerged, NASA demonstrated some of their potential applications in the space flights exploration. Consequently, the industry has started recognizing the commercial aspects of the fuel cells, which, due to the technological barriers and their high production costs, were not economically profitable at that stage of technology [2].

Today, fuel cells of various types have emerged as promising alternative sources of "clean energy" for applications ranging from automotive industry to residential and commercial installations. This has created a need for a class of specialized power converters geared to interface between the fuel cell device and the end-user appliance, often as a battery charger. Specifications for power conversion equipment depend on the fuel cell's physical properties and manufacturing economics.

The most common application areas of fuel cell can be classified in five main groups as shown in Fig. 1 [3].

The cells' output voltage is dependent on the load. So, there is a need to model the fuel cell for optimizing its performance and also for developing fuel cell power converters for various applications.

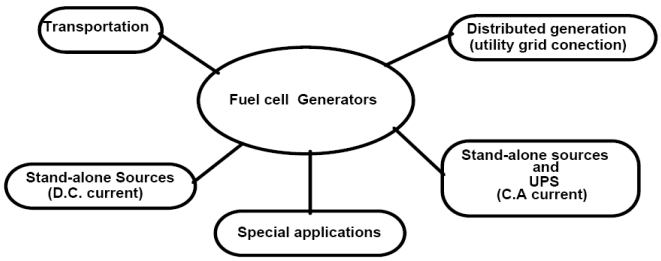

Fig. 1. Classification of fuel cell application.

The proton exchange membrane fuel cell (PEMFC) has been considered as a promising kind of fuel cell during the last 20 years because of its low working temperature, compactness, and easy and safe operational modes. The proton exchange membrane (PEM) fuel cell is very simple and uses a polymer (membrane) as the solid electrolyte and a platinum catalyst.

A fuel cell stack is composed of several fuel cells connected in series separated by bipolar plates and provides fairly large power at higher voltage and current levels.

Up to now different type of models of PEM fuel cell were proposed [4] – [12]. Unfortunately, most of the proposed models cannot be used for practical realization of a fuel cell simulator.

The aim of this paper is to propose a model of a PEM fuel cell which can be extended to a practical realization of a fuel cell simulator that can be used in preliminary design of fuel cell based systems.

II. Description and Operational Principle of the Fuel Cells

The fuel cell is a mini power source generating electrical energy without the combustion stage. The basic physical structure, or building block, of a fuel cell consists of an electrolyte layer in contact with a porous anode and cathode on either side [13]. Porosity of the electrodes enhance the active electrode area hundreds, even thousand times. This fact is very important because electrochemical reactions take place on the electrode surface. Catalyst is incorporated in the electrode microstructure, e.g., platinum, nickel or their alloys which accelerate the speed of electrode's electrochemical reactions

This work was supported by the Ministry of Education and Science of Republic of Macedonia under Project No. 13-936/3-05.

G. L. Arsov is with the Faculty of Electrical Engineering and Information Technologies, Skopje, Republic of Macedonia.

G. Georgievski is with Faculty of Electrical Engineering and Information Technologies, Skopje, Republic of Macedonia.

[13]. The chemical energy is directly transformed into electrical energy and heat when the hydrogen fuel reacts with the oxygen from the air [14], [15]. Water is the sole byproduct of the reaction. The basic electrochemical reaction is the following one [16]:

$$\text{Anode reaction: } H_2 \rightarrow 2H^+ + 2e^- \quad (1)$$

$$\text{Cathode reaction: } \frac{1}{2}O_2 + 2H^+ + 2e^- \rightarrow H_2O \quad (2)$$

$$\text{Overall reaction: } \frac{1}{2}O_2 + H_2 \rightarrow H_2O \quad (3)$$

Looking at the the previous equations, one can get a wrong impression that this process is very simple, but actually the physical and chemical processes happening on each of the electrodes and membrane are rather complex. A schematic fuel cell representation with flow directions of the fuel, reactant and ion current is given in the Fig. 2 [17].

Single fuel cell at no load (e.g. polymere electrolyte fuel cell - PEFC) in ideal case, generates voltage of 1,16 V at the temperature of 80 °C and gas pressure of 1 bar. Loaded fuel

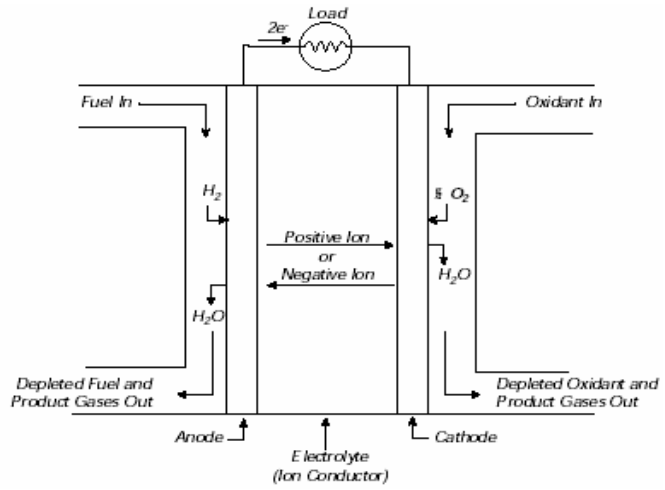

Fig. 2. Operational principle of the fuel cell.

cell at this operational conditions generates 0,7 V. Thereby 60% of the fuel energy is transformed into electrical energy [14]. Maximum emf, E, gained during the hydrogen and air reaction ($H_2 + ½O_2 \rightarrow H_2O$) at the specified values of temperature and pressure can be determined by the following expression:

$$E = -\frac{\Delta g_f}{nF} \quad (4)$$

where Δg_f is Gibbs free energy, n is number of electrons participating in the reaction, and F is the Faraday constant.

In order to use the fuel cell as energy source practically, a number of single fuel cell has to be serially connected (stacked) to gain the higher output voltage.

When the hydrogen is used as a fuel, the pollutants are not products of the reaction. Hydrogen fuel could be produced by electrolysis process using renewable power sources as sun, hydro, geothermal and wind energy. But the hydrogen could be extracted from any hydrocarbons e.g. petrol, naphta, biomass, natural and LPG, methanol, ethanol, etc.

The most often classification of the fuel cell is according to the type of the used electrolyte [13]. So there are five types of fuel cell although basically the same electrochemical reaction takes place in all of them [13]:

- Alkaline Fuel Cell - AFC: AFC operating at 250 °C has an electrolyte of highly concentrated potassium hydroxide KOH while those operating at lower temperatures (120 °C) have lowly concentrated KOH. The electrolyte is retained in an asbestos matrix. Wide spectrum of catalysts is used: Ni, Ag etc. The fuel is limited to non-reactive constituents except for hydrogen.
- Polymer Electrolyte Membrane Fuel Cell - PEMFC: Electrolyte in this fuel cell is ionic membrane (Sulfuric acid polymer) which is excellent ionic conductor. Water is the only liquid in the PEMFC and consequently the problem with the corrosion of PEMFC elements are minimal. Water management is a key factor for PEMFC efficient operation. During the operation the PEMFC the humidity of the membrane is critical which determines the operational temperature of the PEMFC in the range of 60-100 °C. The fuel is hydrogen H_2 enriched gas with no presence of CO (fuel cell poison at low temperatures). Platinum is used as a catalyst
- Phosphoric Acid Fuel Cell - PAFC: Concentrated phosphoric acid (up to100%) is used in PAFC at operating temperatures in the range of 150 - 250 °C. At lower temperatures, phosphoric acid is bad ionic conductor, and catalyst (Pt) poisoning with CO becomes extremely severe. The relative stability of the phosphoric acid is high compared to the other acids, and that is the reason why this acid is operative at high temperatures with small water quantity which make the water management easy. Electrolyte is put up in silicon matrix while the type of the used catalyst is Pt.
- Molten Carbonate Fuel Cell - MCFC: MCFC's electrolyte is combination of alkali carbonates or combination of Na and K, placed in a ceramic matrix made up of $LiALO_2$. Operational temperature of the MCFC is in the range of 600 °C to 700 °C at which the alkali carbonates form highly ionian conductive molten salt. Ni (anode) and nickel oxide (cathode) are used to promote reaction.
- Solid Oxide Fuel Cell - SOFC: The memebrane electrolyte is solid nonporous metalic oxide usually Y_2O_3 - stabilized ZrO_2. Operational temperature is in the range from 650 to 1000 °C where ionic conduction of oxygen ions occurs. Typically anode is made of Co-ZrO_2 or Ni-ZrO_2 cermet and cathode is Sr-doped $LaMnO_3$.

Initial use of the fuel cells was in the NASA's space flights, for power generation and production of fresh water for the astronauts. Today the fuel cells might be used in three categories of aplications: transport, stationary and portable aplications.

AFC is the first modern type of fuel cell developed in the 1960's for the "Apollo" space program. The excellent performances of AFC comparing to the other types of fuel

cells, are due to the active O_2 electrode kinetics and its flexibility to use a wide range of elctrocatalysts. But, pure H_2 has to be used as fuel because CO_2 in any reformed fuel reacts with KOH electrolyte to form carbonate thus reducing the electrolyte's ion mobility. Purification of the fuel is rather expensive and because of that the use of AFC is limited to the space applications where fuel is pure hydrogen. In the NASA's Space shuttle three 12 kW units have been used for 87 missions with 65 000 hours flight time duration.

PEMFC are used in the transport aplications. Exceptionally interesting for this kind of applications is the Direct Methanol Fuel Cell - DMFC. In this type of fuel cell metilacohol (methanol) is directly used as a fuel needing no reformer stage [14]. PEMFC generate electrical energy with high efficiency and power density (180 - 250 mW/cm2) [13]. Also, this type of fuel cells can be used in a small stationary applications for generation of electrical power and heating in the individual houses. The power range is from 2 to 10 kW. This achievement is made by the cost reduction of the materials and manufacturing. Their main advantage is low operating temeperatures 60-100 °C and solid electrolyte. Due to the low operational temperature anode catalyst poisoning with CO is significant especially at higher current densities. In this case the output voltage of the fuel cell becomes unstable and fluctuating. Also due to the low operating temperatures, expensive catalysts have to be used for increasing the speed of the electrochemical reactions (platinum).

PAFC are for the time being the only one commercialized type of the fuel cell. It is relatively simple, reliable and quiet power source with 60% efficiency (with cogeneration). As fuel could be used natural gas. 60 MW of this type fuel cells generators are installed worldwide. The power range of the most of the power stations is between 50 and 200 kW, but also they are constructed in the range between 1 and 5 MW. Operational temperature is around 200 °C, and power density reaches values of 310 mW/cm^2. The PAFC anode is very sensitive to catalyst poisoning even if very small concentrations of contaminants (CO, COS and H_2S) are present. Compromise between the demand for high power density and good operational performances through the life spans of the PAFC should be made. One of the primary targets for the future PAFC development is the extension of the PAFC's life span up to 40 000 hours.

MCFC operates at around 600 °C. At this temperature many of the disadvantages of the lower as well as higher temperature cells can be alleviated with the fact that, for manufacturing MCFC, commonly available materials can be used (utilization of metal sheets reduces fabrication costs), while nickel catalyst is used instead of expensive precious metals. Reforming process takes place within the cell and CO is used directly as a fuel. However, the electrolyte in the MCFC is very corrosive and mobile while the higher temperature influences the mechanical stability and the lifetime of the MCFC materials. An Energy Research Corporation (ERC) in USA has tested a 2MW power supply which operates from 1996 in Santa Clara, Ca.

SOFC electrolyte is solid and cell can be made in tubular, planar or monolithic shape. The solid ceramic construction of the cell alleviates hardware corrosion problems characterized by the liquid electrolyte cells and is impervious to gas cross-over from one electrode to the other. The absence of liquid also eliminates the problem of electrolyte movement and flooding the electrodes. The kinetics is fast while CO is directly usable fuel as in MCFC. Also, as in MCFC, there is no requirement for CO_2 at the cathode. Operational temperature is around 1000 °C which means that the fuel is directly reformed within the cell. Disadvantages of the high operational temperature are the influences on the cell's material properties meaning the different thermal expansion mismatches. Currently two plants (25 kW and 100 kW), produced by Siemens Westinghouse Power Corporation, are installed and they both have cumulative operating time of 9500 hours. The eventual SOFC market is for large stationary fuel cell power supply systems (100 to 300 MW) using natural gas or coal as a fuel.

III. Fuel Cell Characteristics [13], [17], [18]

The fuel cell directly converts chemical energy into electrical energy. The chemical energy released from the fuel cell can be calculated from the change in Gibbs free energy (Δ_{gf}) which is the difference between the Gibbs free energy of the product and the Gibbs free energy of the reactants [18]. The Gibbs free energy is used to represent the available energy to do external work. For the hydrogen/oxygen fuel cell, the basic chemical reaction is given by (3), and the change in the Gibbs free energy can be expressed as:

$$\Delta g_f = g_{f.of.products} - g_{f.of.reactants}$$

$$= (g_f)_{H_2O} - (g_f)_{H_2} - (g_f)_{O_2} \quad (5)$$

The change in Gibbs free energy varies with both, temperature and pressure:

$$\Delta g_f = \Delta g_f^{\,o} - RT_{fc} ln\left[\frac{p_{H_2} p_{O_2}^{\,1/2}}{p_{H_2O}}\right] \quad (6)$$

where $\Delta g_f^{\,o}$ is the change in Gibbs free energy in standard pressure (1 bar) which varies with temperature T_{fc} in Kelvin. The partial pressures p_{H2}, p_{O2} and p_{H2O} of the hydrogen, oxygen and vapor are expressed in *bar*. R is the universal gas constant, 8.31454 J/(kg·K). The value of Δg_f is negative, which means that the energy is released from the reaction.

For each mole of hydrogen, two moles of electrons pass around the external circuit and the electrical work done (charge × voltage) is:

$$W = -2FE \quad \text{(J)} \quad (7)$$

where F is the Faraday constant (96485 C) which represents the electric charge of one mole of electrons and E is the voltage of the fuel cell. The electrical work done would be

equal to the change in Gibbs free energy if the system were considered reversible. Now, the equation (4) can be rewritten as:

$$\Delta g_f = -2FE \tag{8}$$

The reversible open circuit voltage of the fuel cell or "Nertst" voltage of hydrogen fuel cell is [18]:

$$E = -\frac{\Delta g_f}{2F} = \frac{\Delta g_f^{\,o}}{2F} + \frac{RT_{fc}}{2F} ln\left[\frac{p_{H_2} p_{O_2}^{\,1/2}}{p_{H_2O}}\right] \tag{9}$$

$$E = 1.229 - 0.85\times10^{-3}(T_{fc} - 298.15) +$$

$$+ \; 4.3085\times10^{-3} T_{fc}\left[\ln(p_{H_2}) + \frac{1}{2}\ln(p_{O_2})\right] \tag{10}$$

T_{fc} is expressed in Kelvin, and p_{H2} and p_{O2} in atm.

The actual voltage of the fuel cell is less than the value calculated by equation (10). Typical PEM fuel cell performance plot is given in Fig. 3. The differences are result of losses or irreversibilities.

The current density, cell current per cell active area $A_{fc}(cm^2)$, is:

$$i = \frac{I_{st}}{A_{fc}} \tag{11}$$

The fuel cell losses are attributed to three categories: the *activation* loss, the *ohmic* loss and the *concentration* loss.

The voltage drop due to activation loss is dominated by the cathode reaction conditions. The relation between the activation overvoltage v_{act} and the current density is described by the Tafel equation:

$$v_{act} = a\,ln(\frac{i}{i_0}) \tag{12}$$

where, a is a constant and i_0, the exchange current density, is also a constant. Both constants can be determined empirically. For low temperature PEM fuel cell, the typical value of i_0 is about $0.1 mA/cm^2$.

The ohmic loss arises from the resistance of the polymer membrane to the transfer of protons and the resistance of the electrode and the collector plate to the transfer of electrons. The voltage drop that corresponds to the ohmic loss is proportional to the current density:

$$v_{ohm} = i \cdot R_{ohm} \tag{13}$$

R_{ohm} ($\Omega\cdot cm^2$) is the internal electrical resistance. The resistance depends strongly on the membrane humidity and the cell temperature.

The concentration loss or concentration overvoltage results from the drop in concentration of the reactants as they are consumed in the reaction. These losses are the reason for rapid voltage drop at high current densities. The voltage drop due to concentration losses is given by:

$$v_{conc} = i(c_2 \frac{i}{i_{\max}})^{C_3} \tag{14}$$

where c_2, c_3 and i_{max} are constants that depend on the temperature and the reactant partial pressure and can be determined empirically. The parameter i_{max} is the current density that causes precipitation voltage drops.

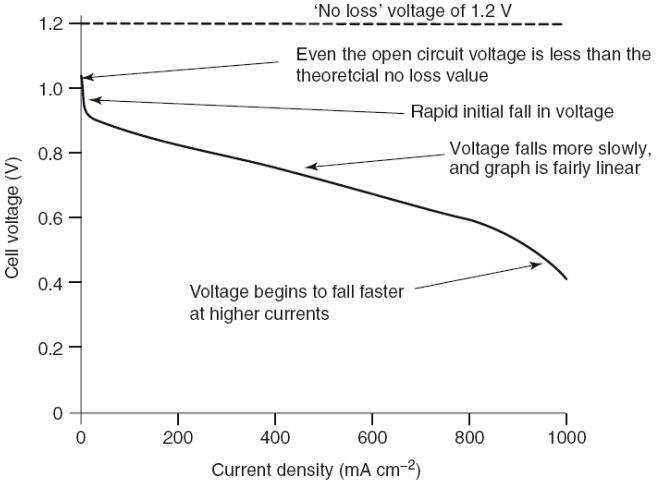

Fig. 3. Graph showing the voltage-current dependence of a typical PEM fuel cell.

By combining all voltage drops associated with all the losses, the single fuel cell operating voltage can be written as:

$$v_{fc} = E - v_{act} - v_{ohm} - v_{conc} =$$

$$= E - a\ln(\frac{i}{i_0}) - [iR_{ohm}] - \left[i\left(c_2 \frac{i}{i_{max}}\right)^{C_3}\right] \tag{15}$$

where, the open circuit voltage E is given by (10).

The fuel cell stack comprises multiple fuel cells connected in series. The stack voltage can be calculated as:

$$v_{st} = n v_{fc} \tag{16}$$

IV. CIRCUIT MODEL OF A PEM FUEL CELL SIMULATOR

The circuit diagram for simulating the fuel cell characteristics, which can be realized for experimental investigations, is composed of two parts: the power circuit and the control circuit.

To achieve appropriate power supplied to the load, the DC-DC buck converter has been proposed as a main power circuit. The microcontroller PIC 16F877 [19] is used to implement the proper fuel cell $\tilde{V}I$ characteristics into the DC-DC converter.

The complete circuit is shown in Fig. 4.

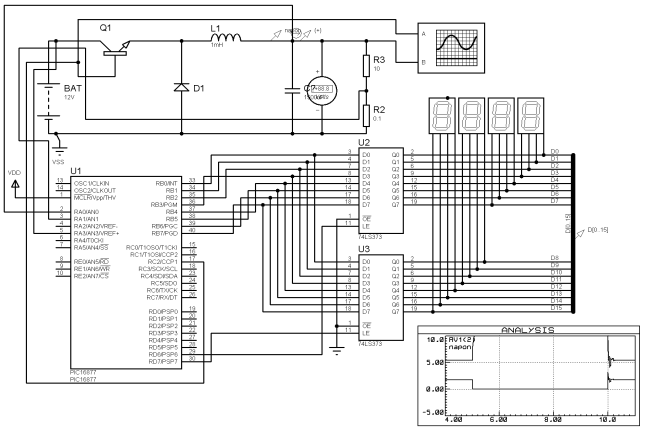

Fig. 4. Proposed circuit model of PEM fuel cell module.

A. Design of the DC-DC buck converter

The main stage of the proposed circuit consists of a classical buck converter shown in Fig. 5.

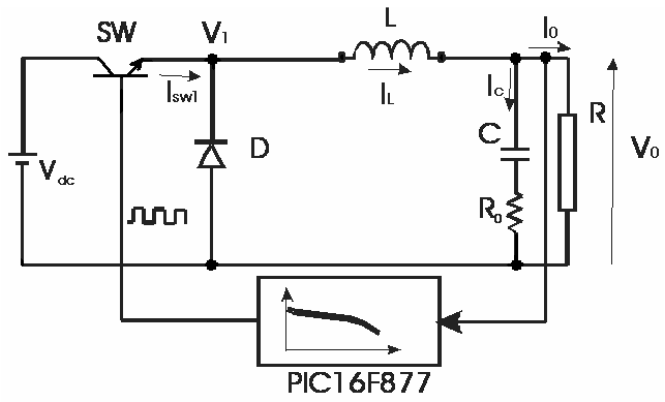

Fig. 5. DC-DC buck converter.

The design procedure of the buck converter is based on the methodology explained in [20].

In general, the output voltage of the buck converter can be defined as $V_0=V_{dc}T_{on}/T$, where T_{on} is the interval during which the switch is ON, and is independent of whatever the switching period T is [20]. The question arises as to whether there is an optimum period and on what basis the period is selected.

The switching losses are proportional to the switching time of the transistor, τ, as shown by (17). The switching time is defined by the turn-on and turn-off intervals during one period of the control signal. Decreasing T results in increased losses and possible necessity for use of large heat sink to keep the switching transistor temperature within desired limits.

$$P_{sw} = \frac{V_{dc} I_o}{2} \frac{\tau}{T} \tag{17}$$

In order to use higher switching frequencies the diode, D, should be specified as ultra fast recovery type, which has reverse recovery time as low as 35 to 50 ns. Thus, the increasing of the switching frequency will decrease the size of the filter elements, L and C, but will contribute to the total losses and to the requirement for a larger heat sink. Optimum switching frequency for this type of circuits is found to be between 25 and 50 kHz.

The values of the inductance L and the capacitance C may be chosen in the following manner.

The value of the inductance L is usually specified in the manner that it's current does not become discontinuous before the DC output current falls to its specified minimum value, which in most cases is one-tenth of the nominal value, or $0.1\times I_{on}$.

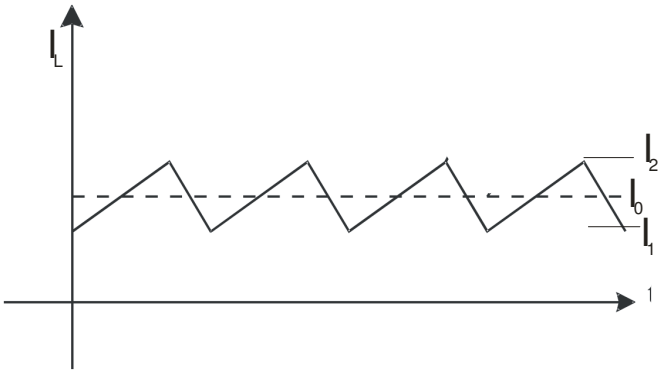

Fig. 6. Inductor current I_L.

The onset of the discontinuous mode occurs at a DC current equal to half the amplitude of the inductor current ramp. For V_{dc} = 12V, I_{on} = 5A, T=40×10^{-6}s, and V_0/V_{dc}=0.5, the inductor L is:

$$L = \frac{(V_{dc} - V_0)T_{on}}{dI} = \frac{(V_{dc} - V_0)T_{on}}{0.2 \cdot I_{on}} \tag{18}$$

$$T_{on} = V_0 T / V_{dc} \tag{19}$$

$$L = \frac{5(V_{dcn} - V_0)V_0 T}{V_{dcn} I_{on}} = 120\mu\text{H} \tag{20}$$

where, V_{dcn} and I_{on} are their nominal values. The inductor must be designed so that it does not saturate at DC current of $1.1I_{on}$. The selected inductor can tolerate higher output currents, than the specified I_{on}, if the used core is designed not to enter the saturation region at these higher currents. The only restrictions on maximum currents in the buck converter are the increased

DC and switching losses in the switching transistor.

The value of the capacitance C is chosen to meet the output voltage ripple specifications. It is not an ideal capacitor. A real capacitor has the parasitic resistance R_0 and inductance L_0 in series with its capacitance. These are referred to as the equivalent series resistance (*ESR*) and equivalent series inductance (*ESL*). Below 300 kHz, L_0 can be neglected and output ripple is determined by R_0 and C. There are two ripple components, due to C and R_0. The ripple component due to *ESR* is proportional to the $(I_2–I_1)$, the peak to peak inductor ramp current, as shown in Fig. 6. The ripple component due to C is proportional to the average current value. For the most frequently used types (aluminum electrolytic capacitors) over a large range of voltage ratings and capacitance values, the product R_0C tends to be constant. Usually, its range is from $(50–80)\times10^{-6}$. Let's assume that the resistive ripple component V_{rr} is 0.05V peak to peak. Then, we may write down: $V_{rr} = 0.05 = (I_2–I_1)R_0$, or, for $I_2 – I_1 = 1$ A, we will obtain $R_0 = 0.05\ \Omega$. Now, for $R_0C = 50\cdot10^{-6}$:

$$C = 50\cdot10^{-6}/0.05 = 1000\mu\text{F} \qquad (21)$$

The capacitive ripple voltage V_{cr} is produced from the average value of current $(I_2–I_1)/4 = 0.25$A. This current produces a ripple voltage across C described by (22):

$$V_{cr} = \frac{\Delta I \cdot t}{C} = \frac{0.25 \cdot 40 \cdot 10^{-6}}{1000 \cdot 10^{-6}} = 0.01\,\text{V} \qquad (22)$$

The total peak to peak capacitive ripple voltage is 0.01V. This may be ignored, compared with the ripple voltage as a result of R_0.

The calculation of L and C, as well as the selection of the bipolar transistor and the diode, should be reconsidered for any different case, depending on the voltage and current capabilities of the simulated fuel cell. For simulation purposes this can be done by the software but when using hardware solution this components should be physically changed.

B. The control algorithm

The microcontroller PIC16F877 is proposed for controlling the proper work of the power stage. In general, this is a "computer on a chip" that can be programmed and reprogrammed by the end user.

The PIC16F877 includes 10-bit multi-channel Analog-to-Digital converters and two PWM modules by which pulse width modulation can be easily implemented. The Analog-to-Digital converter is used to convert the analog values of the output voltage and current into digital for further processing. Using 10-bit A/D converter, the discretization error will be less than 0.1%. For example, if the ideal no load voltage is selected to be $V_{dc} = 12$ V, the discretization error will be less than 0.01 V. The PIC16F877 can be easily programmed using its instruction set consisted of 35 instructions. The instruction cycle of 200 ns allows us very good real time operation.

Although the simulated curve can be calculated using relations (8) – (16), or by using some of the referred simulation models, here we use the measured polarization curve, of a single fuel cell, at specified conditions which is implemented in the PIC memory. The values can be modified depending of the stack current and voltage capabilities, as well as the working temperature.

In this case we have implemented the polarization curve for a single PEM fuel cell with "no loss" voltage of 1.2V and maximum current 1A, according to the Fig. 3. The working temperature is assumed to be 80 ^{o}C, and the pressure is standard (100 kPa).

The control algorithm is shown with its block diagram in Fig. 7. The actual output current, $I_{0(t)}$, and voltage, $V_{0(t)}$, are converted to 10-bit digital numbers using the A/D module. After comparison with previous values and with the values defined by the implemented polarization the command sequence for driving the PWM module is generated. Now the PWM module generates pulses for proper driving of the switching transistor thus controlling the output voltage V_0.

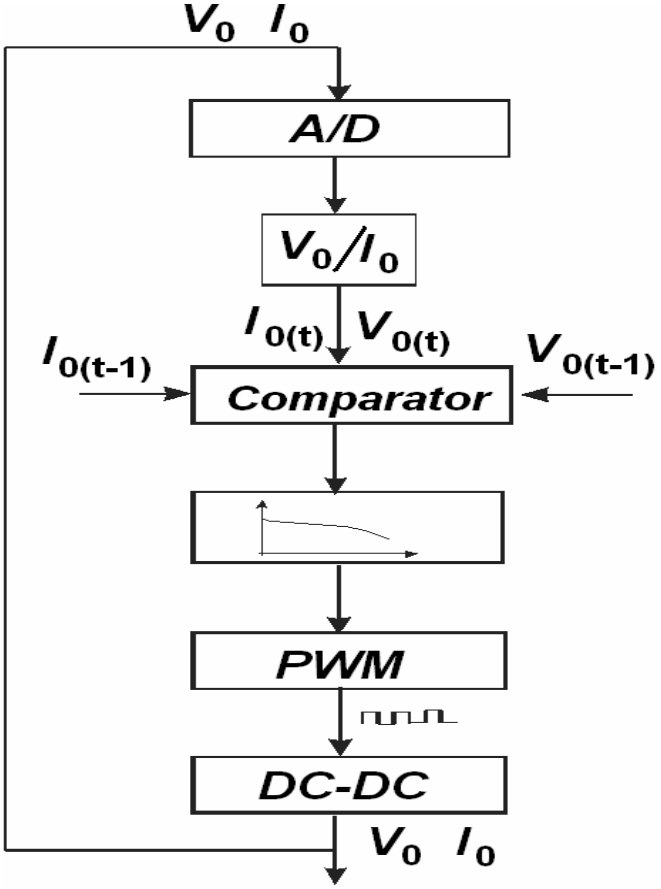

Fig. 7. Block diagram of the control algorithm.

V. Simulation Results

The extensive simulations of the proposed model have been performed using the PROTEUS PROFESSIONAL. Some of the results are shown below.

The schematic used to obtain the dynamic characteristics is shown in Fig. 8.

First, we have increased the ideal stack voltage to 12 V, and

the active cell area by 5 (to support the current of 5 A). These values are multiples of the initial polarization characteristics implemented in the PIC memory. The microcontroller PIC16F877 measures current I_0 and voltage V_0 and with the software, implemented in its memory, creates PWM pulses for driving the buck converter. The period of the PWM pulses is constant and was chosen to be 25 kHz. The pulse width is controlled by the implemented polarization curve and measured values of the output current, I_0, and voltage, V_0. The output voltage varies from 12 V, at system idle, to about 5V, at rated current of 5 A. The simulation results of the static *V–I* characteristics are shown in Fig. 9.

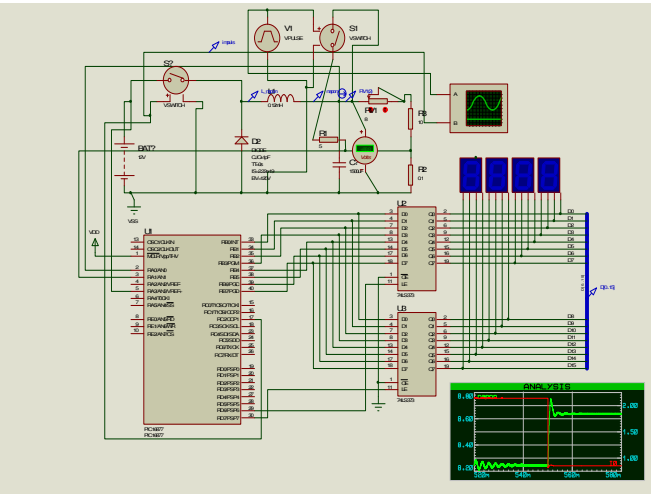

Fig. 8. The schematics presentation of the simulated circuit in PROTEUS PROFESSIONAL.

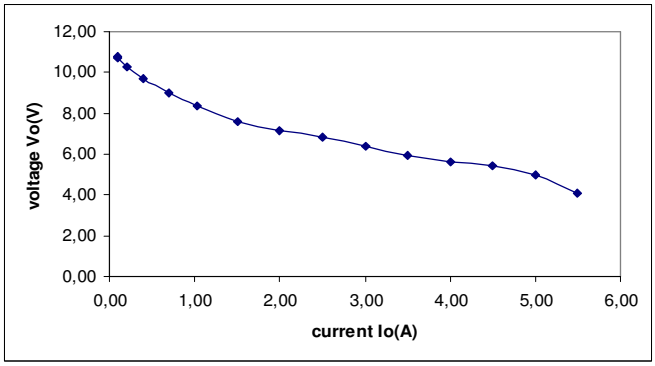

Fig. 9. Simulated V-I characteristic for PEM fuel cell model (12V/5A).

The dynamic response of the model is very fast and follows the polarized *V–I* curve of a PEM fuel cell. The step change of the load resistance, from 50 to 2 Ω, resulted in increasing the current to 2.2 A, and the decreasing the output voltage to 6.6 V. The simulation results are shown in Fig. 10.

To examine the operation of our model the simulation results are compared with measured ones, of a commercially available fuel cell system.

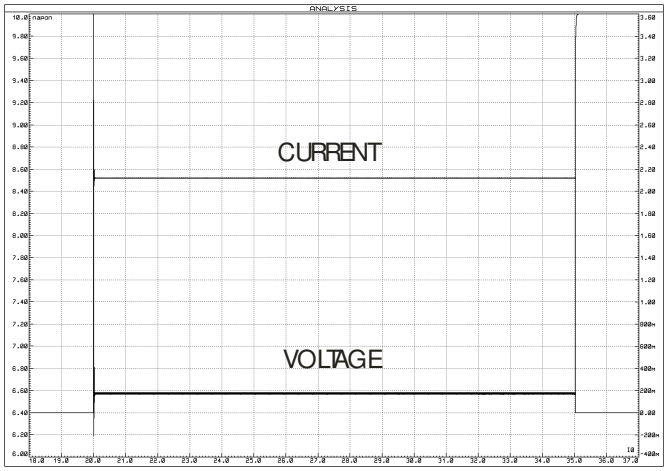

Fig. 10. Simulated waveforms for a dynamic behavior of a PEM fuel cell model.

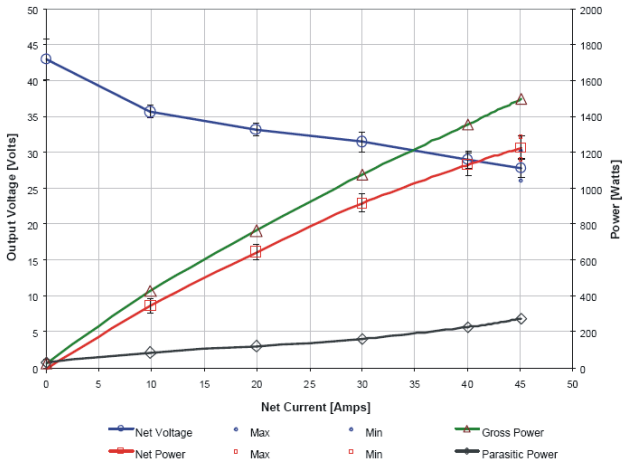

(a)

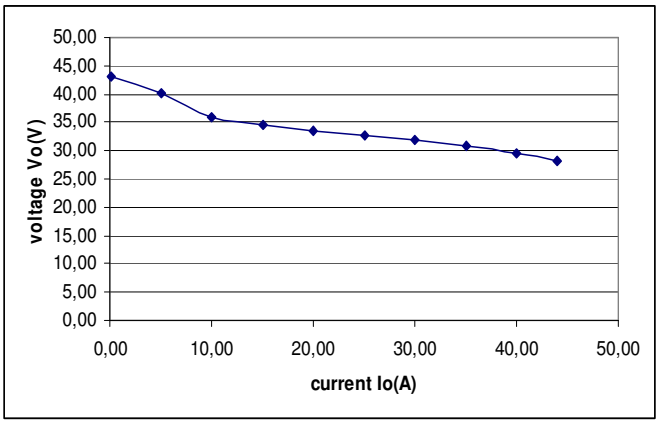

(b)

Fig. 11. (a) V-I characteristics of a PEM fuel system obtained from experiment [21], (b) Simulated V-I characteristics of DC-DC converter for maximum voltage 48V and maximum current 45A.

In Fig. 11-(a) we show the polarization characteristics of the Nexa™ system [21]. The output power ranges from zero at system idle to 1200 watts at rated power. The output current varies from zero to 46 A. The output voltage changes with operating load according to the polarization characteristics of the fuel cell stack. Normal idle DC

voltage of the Nexa™ system is approximately 43 V. At rated power, the Nexa™ system DC output voltage ranges from 26 to 29 V.

In Fig. 11-(b) we show the simulated *V–I* characteristics of the DC–DC, buck converter based, PEM fuel cell model adapted to the Nexa™ system. It can be seen that the characteristics corresponds very well to the measured one given in Fig. 11-(a).

VI. CONCLUSION

A preliminary design of a PEM fuel cell model, based on DC-DC buck converter, suitable for hardware realization has been presented. Due to the digital nature of the control system, it is possible to make quick changes to the mathematical model, thus avoiding changes in the system hardware in most cases. The hardware changes affect only the power stage, when larger stack current and/or voltage have to be obtained. The temperature and pressure characteristics can be easily implemented in this model.

The proposed model can be used in the design process of fuel cell power systems, during simulation or practical realization stages. When realized in practice, this PEM fuel cell simulator can be also used to test power systems designed to interact with PEM fuel cells, in order to prevent stack degradation caused by the electric behavior of the system. Foreseen benefits of this model are the ability to work without reagents in a non-specialized environment, in a reproducible way and with a faster start-up/turn-off operation.

The proposed model has been tested by simulation using the PROTEUS PROFESSIONAL. The model is validated by comparing the simulation and experimental results obtained on a commercial PEM fuel cell module.

By realizing the hardware and further development of the software, using the equations (8) – (16), this model can be transformed into real fuel cell emulator.

A conclusion section is not required. Although a conclusion may review the main points of the paper, do not replicate the abstract as the conclusion. A conclusion might elaborate on the importance of the work or suggest applications and extensions.

REFERENCES

[1] Sharon Thomas, Marcia Zalbowitz, "Fuel Cells – Green Power," *Los Alamos National Laboratory, New Mexico*, 1999.

[2] "Fuell Cells Fact Sheet," *Enviromental and Energy Study Institute, Washington DC*, February 2000.

[3] Y. R. Novaes, I. Barbi, "Low Frequency Ripple Current Elimination in Fuel Cell Systems", *2003 Fuel Cell Seminar Proceedings,*" Miami, November, 2003, pp. 21-26.

[4] S. Yerramalla, A. Davari, A. Feliachi, "Dynamic modeling and analysis of polymer electrolyte fuel cell", *Proc. IEEE Power Engineering Soc. Summer Meeting*, vol. 1, 2002, pp. 82–86.

[5] J.B. van der Merwe, C. Turpin, T. Meynard, B. Lafage, "The installation, modeling and utilization of a 200W PEM fuel cell source for converter based applications", *Proc. IEEE Power Electronics Specialists Conference, 2002*, pp. 333–338.

[6] K. Dannenberg, P. Ekdunge, G. Lindbergh, "Mathematical model of the PEMFC", *J. Appl. Electrochem.* 30 (2000) pp. 1377–1387.

[7] A. Kazim, H.T. Liu, P. Forges, "Modeling of performance of PEM fuel cells with conventional and interdigitated flow fields", *J. Appl. Electrochem.* 29 (1999) pp. 1409–1416.

[8] W. Turner, M. Parten, D. Vines, J. Jones, T. Maxwell, "Modeling a PEM fuel cell for use in a hybrid electric vehicle", *Proc. IEEE Vehicular Technology Conference*, 1999, pp. 16–20.

[9] R. Gemmen, P. Famouri, "PEM fuel cell electric circuit model", *Proc. of the Power Electronics for Fuel Cells Workshop*, 2002.

[10] D. Yu, S. Yuvarajan, "Electronic circuit model for proton exchange membrane fuel cells", *Journal of Power Sources* 142 (2005). pp. 238–242.

[11] A. Capel, J. Calvente, R.Giral1, H. Valderrama-Blavi, A. Romero, and L. Martínez-Salamero, "Modeling of a Fuel Cell as an Energy Source Power System*" Proc SAAEI* 2006, pp. 64-68.

[12] G. L. Arsov, "Parametric Pspice Model of a PEM Fuel Cell" *Electronics,* Vol. 11 No. 1-2*,* FEE - Banja Luka, Dec 2007, pp. 99-103.

[13] National Energy Technology Laboratory, "*Fuel Cell Hand Book*", sixth ed., 2002, pp. 2.1–2.20.

[14] Sharon Thomas, Marcia Zalbowitz, "Fuel Cells – Green Power," *Los Alamos National Laboratory, New Mexico*, 1999.

[15] "Fuel Cells Fact Sheet," *Environmental and Energy Study Institute, Washington DC*, February 2000.

[16] Andrew R. Balkin, "Modeling a 500 W Electrolyte Membrane Fuel Cell," *University of Technology, Sydney*, June 2002.

[17] J. Larminie, A. Dicks "*Fuel Cell Systems Explained*", Wiley, 2003.

[18] Jay T. Pukrushpan, Anna G.. Stefanopouplu, Huei Peng "*Control of Fuel Cell Power Systems*", Springer, 2005.

[19] Microchip, *PIC16F87X Data Sheet*.

[20] Abraham I. Pressman "*Switching Power Supply Design"*, McGraw-Hill, 1998.

[21] *Ballard Power System "NexaTM Power Module Integration Guide", 2002*.